Analog Feedback Controller for MEMS Microphone

Design Group 32

Wesley Chiu, EE
Andrew Steinmann, EE
Adam Hess, EE, Music

Faculty Advisor: Ron Miles, Eva Wu
Sponsor: Binghamton University

April 28, 2010

Submitted in partial fulfillment of the requirements of ME 494/EECE 488 in the Spring Semester of 2010.

Thomas J. Watson School of Engineering and Applied Science
State University of New York at Binghamton

Abstract

Currently a MEMs microphone is being developed for next generation hearing aid applications. The microphone is modeled after the ears of *Ormia ochracea* fly which will allow a micro-scale microphone to not only detect sound pressure, but the direction which the sound is coming from as well. Although the very small size is desirable to reduce thermal noise, it significantly reduces the damping ratio which causes an undesirable resonant peak. The resonant peak creates a ringing noise that is unacceptable for a hearing aid application. In order to correct this resonance, feedback will be added to adjust the closed loop system poles to remove the resonance and shape the closed loop frequency response. This paper describes the design process used to develop and implement the proper feedback controller as well as potential problems in the feedback design. An initial feedback controller is proposed and analyzed using Matlab and PSpice. Matlab simulations are performed to confirm the validity of the design and PSpice simulations are used to test the analog circuit realization of the controller. The controller has been prototyped on a breadboard and has been tested using the laser vibrometer sensing mechanism.

I. Introduction

The MEMs microphone currently being developed has some clear advantages over the current generations of hearing aids. The *Ormia ochracea* fly has the unique ability to sense the direction of sound as well as the sound itself. Using the fly's sound sensing capability as motivation, a MEMs microphone was mechanically modeled after the ears. Figure 1 show the mechanical interpretation of the *Ormia ochracea* ears. The microphone rotates around a pivot point in response to sound excitation. This simple mechanical system has the potential to replace current hearing aid microphones for several reasons. One major improvement of the MEMs microphone over current hearing aid microphones is the significantly lower noise floor. The lower noise floor not only allows the user to hear more quite sounds, but also reduces the magnitude of electronic noise. Another improvement of the MEMs microphone is directional sensing aspect. Current hearing aids have poor performance in noisy environments because the hearing aids amplify all the noise. The MEMs microphone is capable of detecting what direction noise is coming from and may reduce background noise and allow the user to focus on what they would like to hear. For example if the user is sitting in a noisy restaurant the MEMs microphone may be able to reduce the background noise and enable the user to more easily carry a conversation with the person across the table.

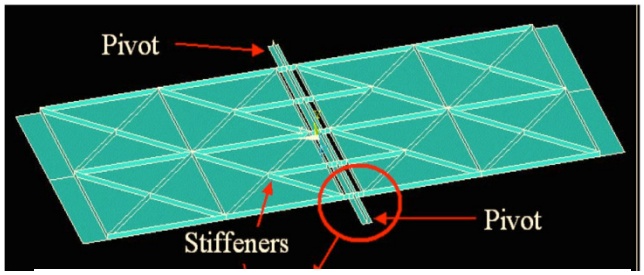

Figure 1 : Microphone

One problem encountered in the development process is creating a small device that does not have a large resonance. One way to decrease the resonance would to increase the stiffness, but that would result in a larger device. The larger device may remove the resonant peak, but the size required to do that may be significantly larger. In addition to the size trade off, the device's

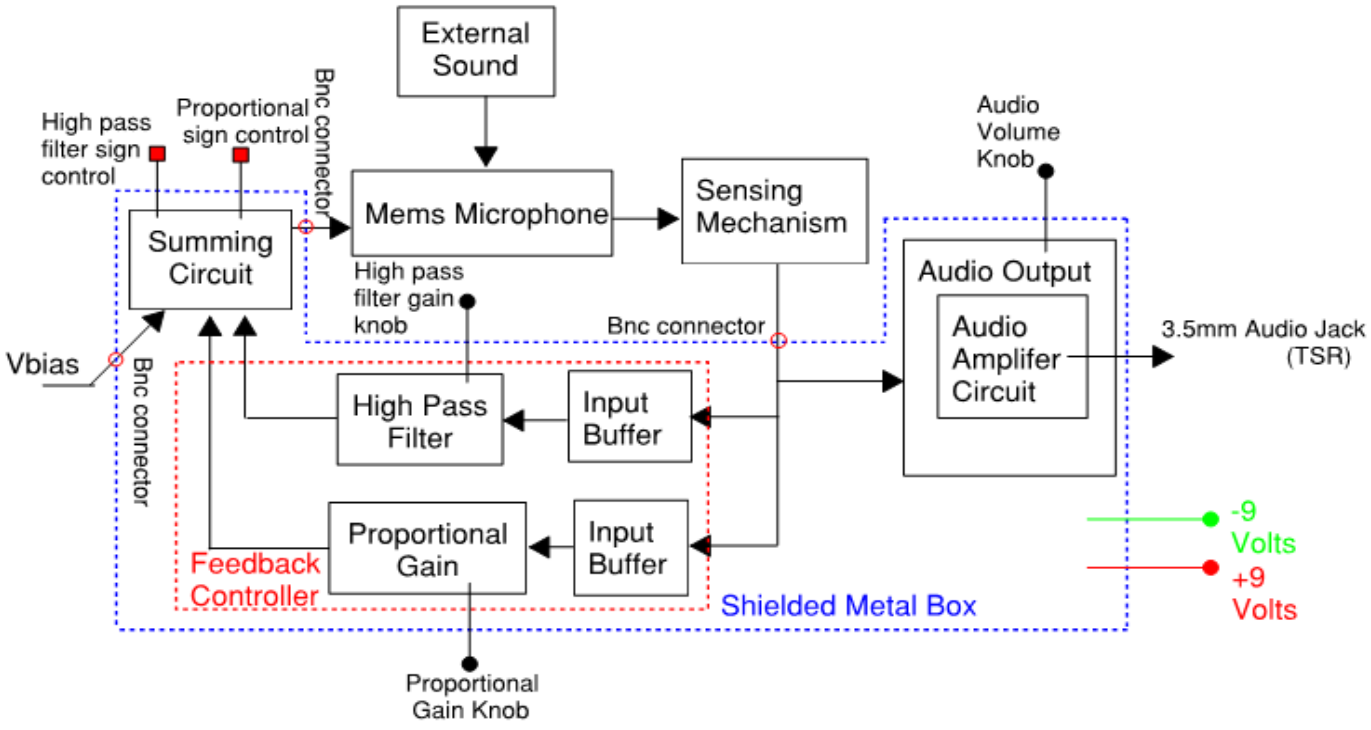

Figure 2: Overall System Block Diagram

thermal noise is related to the size. Therefore by increasing the size significantly, there is a significant increase in noise. Since one of the desirable traits of the microphone is the lower noise floor, this option is not ideal. Another option is to introduction feedback to change the system poles. This option requires additional circuitry, but only slightly hinders the microphone's noise floor. Introducing feedback is the more ideal solution because it does not increase the noise floor significantly and it can remove the resonance while shaping the frequency response.

Figure 2 is the overall block diagram of the microphone and feedback controller. A proportional-derivative controller is chosen to allow flexibility when selecting the desired closed loop system poles. The PD controller's gains have been calculated to a set value, but will be able to change the magnitude and sign in order to account for variations of microphones. The derivative segment of the controller is implemented using a practical high pass filter instead of a pure differentiator. The bias voltage as well as the proportional and derivative signals are summed together using a summing circuit and output the control effort which is applied to the microphone. In addition to the PD controller circuit, there is also an audio amplifier circuit which will allow the user to hear the outputted sound via headphones. The PD controller circuit and audio amplifier will be powered using two 9 volt batteries to provide positive and negative rails required by the op-amps. The controller and audio circuit will be enclosed in a metal chassis to reduce electromagnetic interference and allow the circuit to be transported easily. BNC connectors will be used to interface between the microphone's sensing mechanism and the controller. The audio output will be the standard TRS audio jack to allow all standard headphones to be used to hear the microphone's output.

II. Analysis of problem

As mentioned in the introduction, the MEMs microphone currently has a resonant peak caused by the under damping. In order to correct the resonance the problem must first be analyzed mathematically using the differential equation of the microphone. Equation 1 is the general differential equation associated with motion of rotation of capacitive microphones.

$$I\ddot{\theta} + c_t\dot{\theta} + k_t\theta = M + \frac{V^2}{2}\cdot\frac{\partial C}{\partial \theta} \quad (1)$$

The mass moment of inertia (I), the torsional stiffness (k_t), and the torsional dashpot constant (c_t), are constants associated with each microphone. The moment of the microphone's diaphragm, *M*, is one of the microphone's 'inputs'. The other 'input' of the microphone is a voltage that is converted to a moment by the properties of the microphone. Since the sensing mechanism outputs a voltage and the microphone is able to accept a voltage input, a feedback controller may be added to correct undesirable traits inherent of the microphone's small size. Although a voltage input may be applied, the voltage is squared and multiplied by the derivative of the capacitance with respect to the diaphragm's rotation. This presents two problems, how to use a squared voltage input to successfully introduce feedback and how to approximate $\frac{\partial C}{\partial \theta}$.

One way of handling the nonlinear voltage input is to apply a bias voltage in addition to the feedback voltage. The bias voltage sets a operating point that the microphone will rotated about. By breaking V into V_b+V_f Equation 1 can be rewritten as:

$$I\ddot{\theta} + c_t\dot{\theta} + k_t\theta = M + \frac{{V_b}^2 + 2V_bV_f + V_f^2}{2} \cdot \frac{\partial C}{\partial \theta} \quad (2)$$

The next simplification made is to break θ into two parts, the operating point, γ_0, and rotation due to sound, δ. If only small amounts of rotation caused by sound are considered, such that $V_f << V_b$ and V_f^2 is small the equation becomes:

$$I\ddot{\delta} + c_t\dot{\delta} + k_t\delta = M_s + V_bV_f \cdot \frac{\partial C}{\partial \theta} \quad (3)$$

Using Equation 3 conventional linear controller design can be used. A Taylor series expansion using the first three terms is used to approximated $\frac{\partial C}{\partial \theta}$. The constants necessary for this approximation are obtained experimentally using a laser vibrometer. Assuming that $\frac{\partial C}{\partial \theta}$ is relatively constant around the operating point, it can also be considered constant in the design. Using the Taylor approximation and assuming that $\frac{\partial C}{\partial \theta}$ is relatively constant leads to the final linearized equation:

$$I\ddot{\delta} + c_t\dot{\delta} + k_t\delta = M_s + AV_bV_f \quad \text{where } A \approx \frac{\partial C}{\partial \theta} \quad (4)$$

III. Frequency Domain Analysis

In order to devise a solution that will successfully remove the resonant peak it is imperative to analyze the problem in the frequency domain. The blue line in Figure 1 shows the open loop frequency response of the MEMs microphone. The resonance which occurs at approximately 1600 Hz will cause a ringing sound at that frequency. The ideal microphone frequency response is a band pass, passing frequencies from 20 Hz to 20 kHz with a relatively constant gain. red line in Figure 3 is the bode plot of the ideal/desired closed loop frequency response.

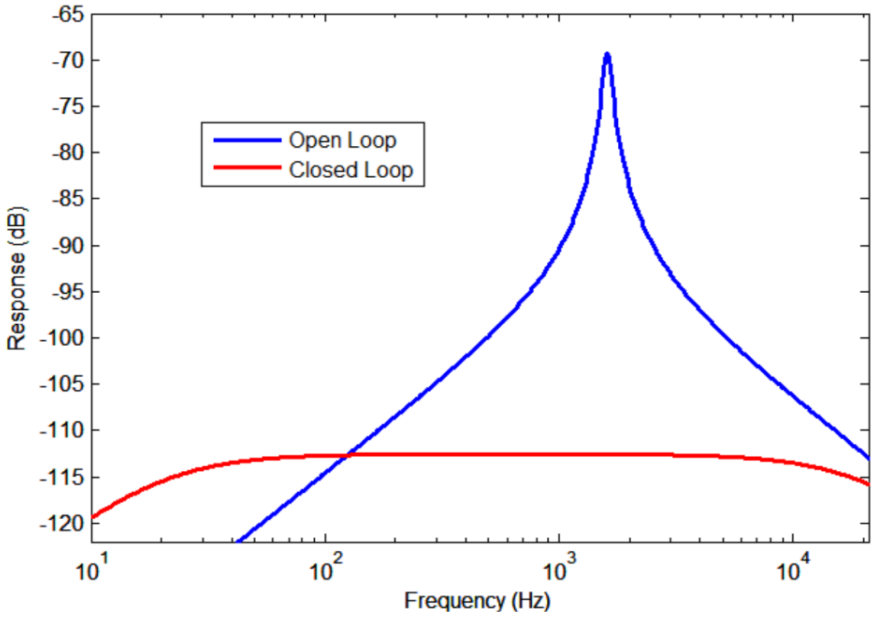

Figure 3: Frequency Response of Open Loop and Closed Loop System

IV. S Domain Controller Design

The first step in the design of a feedback controller is to derive an equation for the desired closed loop system. In this case the desired closed loop system is a band pass from 20 Hz to 20 kHz therefore the system must contain a zero at 0 Hz, a pole at 20 Hz and another pole at 20 kHz. Using these guidelines the ideal/desired closed loop response is determined to be:

$$G_{desired}(s) = \frac{k \cdot s}{(s+2\pi \cdot 20)\cdot(s+2\pi \cdot 20000)} = \frac{k \cdot s}{s^2+2\pi \cdot 20020 \cdot s+4\pi^2 \cdot 400000} \quad (5)$$

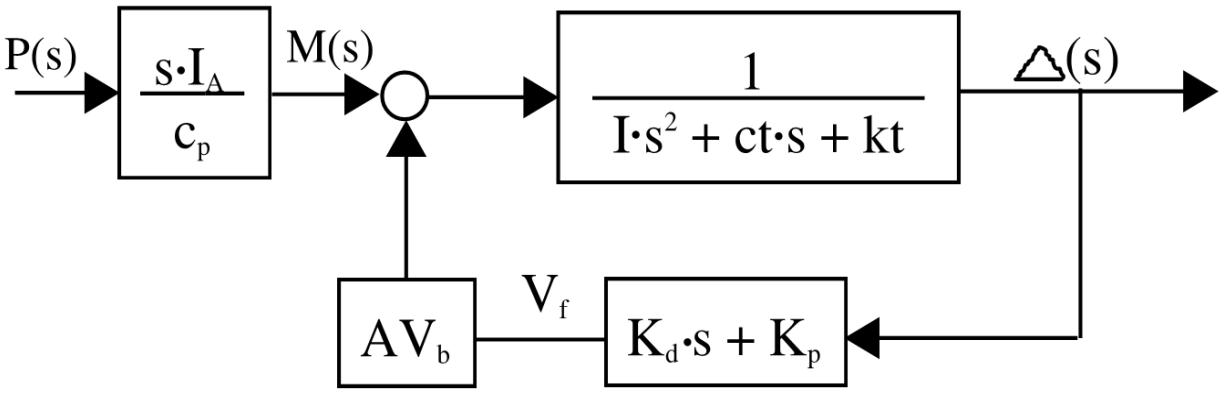

Figure 4: Linearized Control System Block Diagram

Next an arbitrary controller is introduced with an s term and a constant term, or a PD controller. By selecting appropriate gains for the PD controller the poles can be set the desired poles. Figure 4 shows the linear control system model of the microphone plus feedback system. Since the bias voltage and the derivative of our capacitance with respect to the rotation have both been determined to be constant in the linearized model they can simply be treated as a gain in the feedback channel. Using block diagram reduction the diagram in Figure 2 can be reduced to:

$$G_{cl}(s) = \frac{I_A \cdot s/c_p}{I \cdot s^2+(ct-AV_bK_d)\cdot s+(k_t-AV_bK_p)} \quad (6)$$

Finally to obtain the proper gains for the feedback controller (K_p and K_d), the closed loop transfer function is set equal to the desired transfer function. This yields the results:

$$K_d = \frac{c_t - I \cdot 2\pi \cdot (20020)}{AV_b} = 4.496 \quad and \quad K_p = \frac{k_t - I \cdot 4\pi^2 \cdot (400000)}{AV_b} = -3072.3 \quad (7)$$

V. Realistic Differentiator Design

After calculating the ideal controller parameters, it must be considered how to physically realize the system. Implementing a pure differentiator using an op amp presents stability problems and amplifies high frequency noise. A realistic differentiator must include a pole to prevent high frequency noise from being amplified and improves stability. Equation 8 is the transfer function of generic high pass filter. Putting a pole after the frequency range of interest

will effectively differentiate until the pole distorts the phase. Therefore this pole must be high enough to not affect the system.

$$H(s) = \frac{k \cdot s}{s + \omega_c} \quad (8)$$

The additional pole presents other issues that must be corrected for the controller to be effective. Specifically, the derivative gain must be multiplied by the additional pole in order to provide the same control effect. Figure 5 shows the bode plots of a true differentiator, a high pass filter with gain equal to the previously calculated derivative gain, and a high pass with the calculated gain times the additional pole. The green line's gains are significantly less than the true differentiator and thus will not have results in the same closed loop system. Using this knowledge the high pass filter gain is determined to be $\omega_c * K_d$, where K_d is equal to the calculated derivative gain from the S-Domain Design section and ω_c is the corner frequency of the high pass filter.

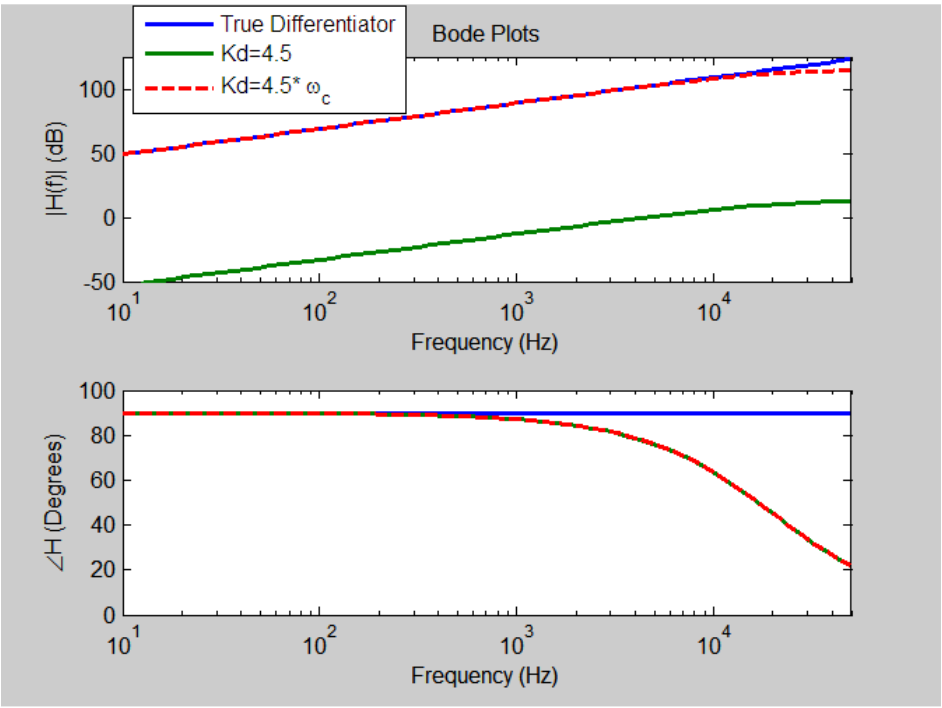

Figure 5: Differentiator & High Pass Filter Comparison

The next issue that needs to be considered for the high pass filter is the gain required to emulate the true differentiator. The overall high pass filter gain is very sensitive to the selection of the corner frequency, but the corner frequency has some constraints. The corner frequency must be large enough to be outside of the bandwidth of the system, but cannot be too large such that the gain is unobtainable. Figure 6 is a plot of the closed loop system poles as a parametric function of the cutoff frequency. Although the values converge to the correct closed loop poles of 20 Hz and 20 kHz the effective gain required is over a million. Even with the estimated sensor gain of 1000, this gain is not close to being feasible. In spite of using the lowest possible corner frequency of 20 kHz, the gain required is 565486 resulting in a gain of 565.5 with the sensor gain. This implies that with a system bandwidth of 20 kHz, the controller is not a realistic goal and the requirements need to be reconsidered.

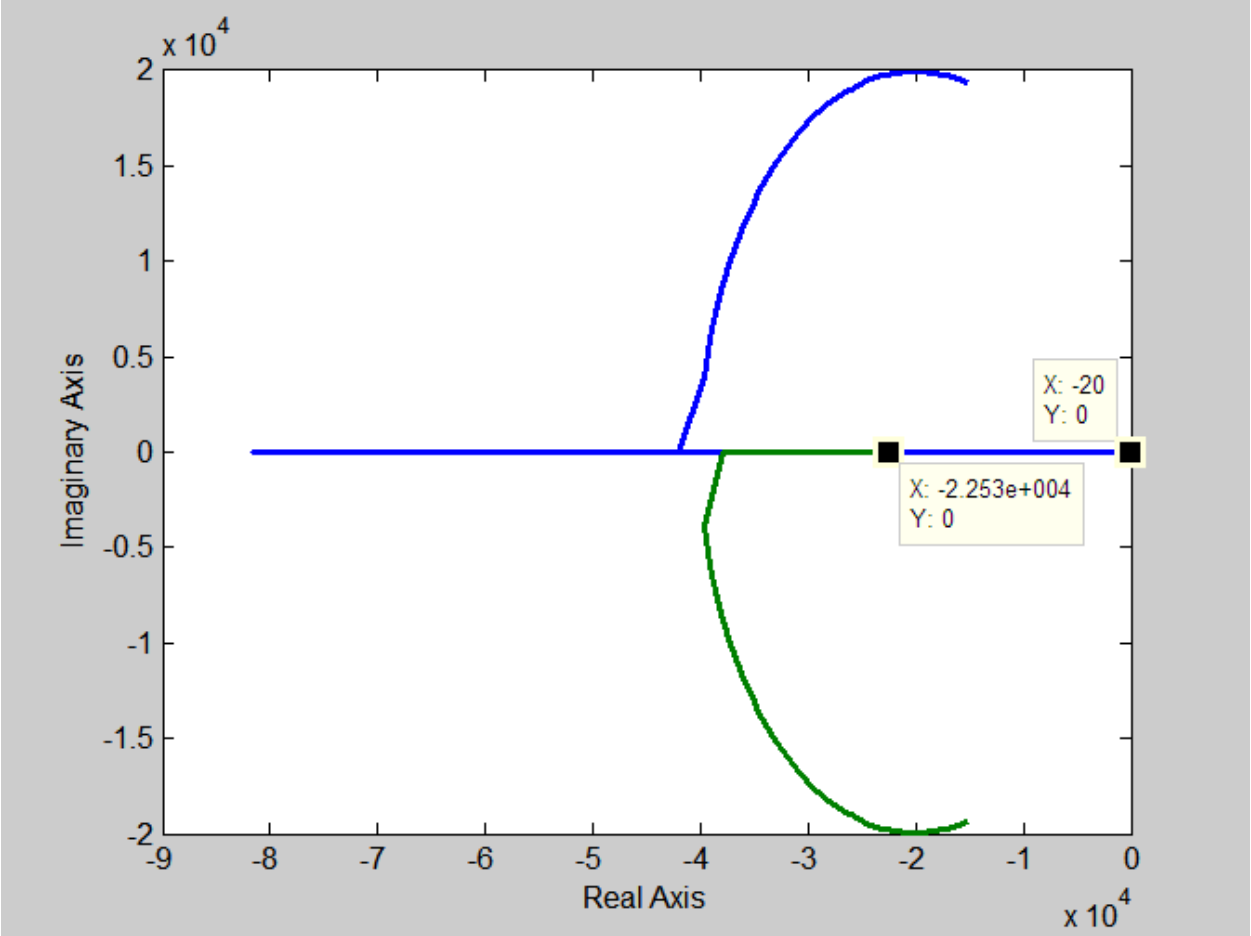

Figure 6: Closed Loop System Poles

The additional pole required to make the system feasible is causing the derivative gain to become unobtainable. This situation requires the reanalysis of the objective of the project as a whole. The MEMS microphone's goal is to provide low noise microphones for hearing aids. Obviously people that use hearing aids have impaired hearing and most likely have lost their higher frequency hearing capability. Following this thought process, it is determined that the bandwidth of the system can be lowered without significant impact on its final use. If the system bandwidth is lowered then the pole of the high pass filter may be lower as well, thus reducing the derivative gain. This tradeoff between bandwidth and gain is required to prove that feedback is capable of improving the frequency response of the microphone. A new bandwidth of 8 kHz was determined to sufficient for the purposes of this project.

Since the corner frequency has a much greater impact on the closed loop system, the design approach must change accordingly. Taking into consideration gain bandwidth product and the rails of the system, the high pass filter gain is set to 60. The cutoff frequency is systematically altered to optimize the closed loop frequency response and the proportional gain remains the same. After many iterations, it was determined that a cutoff frequency of 8.5 kHz should provide sufficient bandwidth using reasonable gains. Figure 7 is the bode plot of the expected closed loop system using realistic controller gains. Although there is a slight bump at around 4 kHz the bandwidth of the system still satisfies the refined requirements. Thus the final design parameters of the controller are K_d=60, K_p=-4.7 and f_c=8.5 kHz.

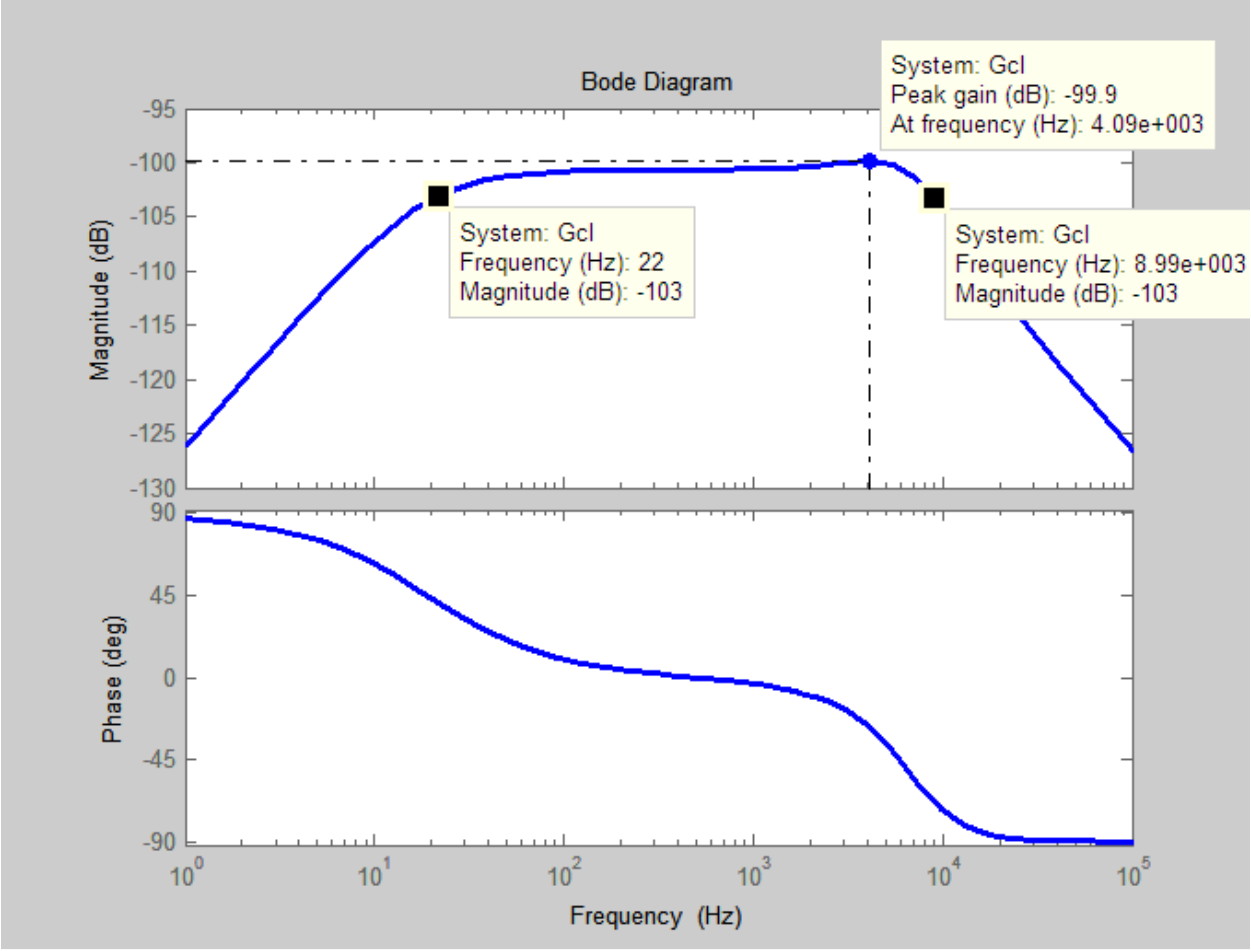

Figure 7: Refined Closed Loop System Response

VI. Notch Filter

An attempted to reduce the large gains of the differentiator was to introduce a shallow notch filter before the controller. The filter needed to have a wide and shallow notch to account for variations in the microphones. This would lower the microphones frequency response peak marginally before the signal enters the controller and therefore allow for lower gains.

A circuit to create a shallow notch filter with wide flexibility can be made from the Twin-T filter configuration. This configuration has a transfer function and configuration of Equation 9.

$$\frac{vo}{vi}=\frac{s^3+s^2\frac{1}{C1}\left(\frac{1}{R1}+\frac{1}{R2}\right)+s\frac{1}{C1R1R2}\left(\frac{1}{C3}+\frac{1}{C2}\right)+\frac{1}{C1C2C3R1R2R3}}{s^3+s^2\left(\frac{1}{C1R1}+\frac{1}{C1R2}+\frac{1}{C2R2}+\frac{1}{C2R3}+\frac{1}{C3R2}\right)+s\left(\frac{1}{C2R3C1R1}+\frac{1}{C2R3C1R2}+\frac{1}{C3C1R1R2}+\frac{1}{C2C1R1R2}+\frac{1}{C2C3R3R2}\right)+\frac{1}{C1C2C3R1R2R3}} \quad (9)$$

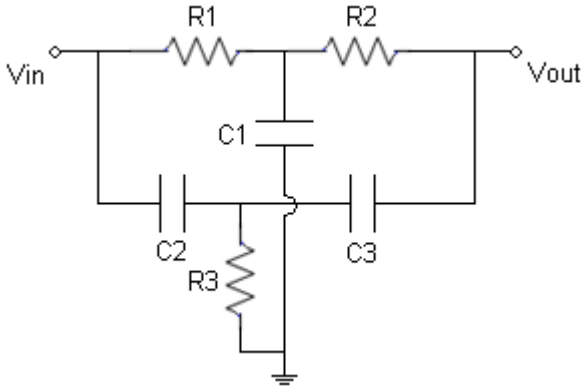

Figure 8: Twin T Notch Filter Configuration

Using this transfer function, a shallow notch filter with the following magnitude and phase was created in simulation:

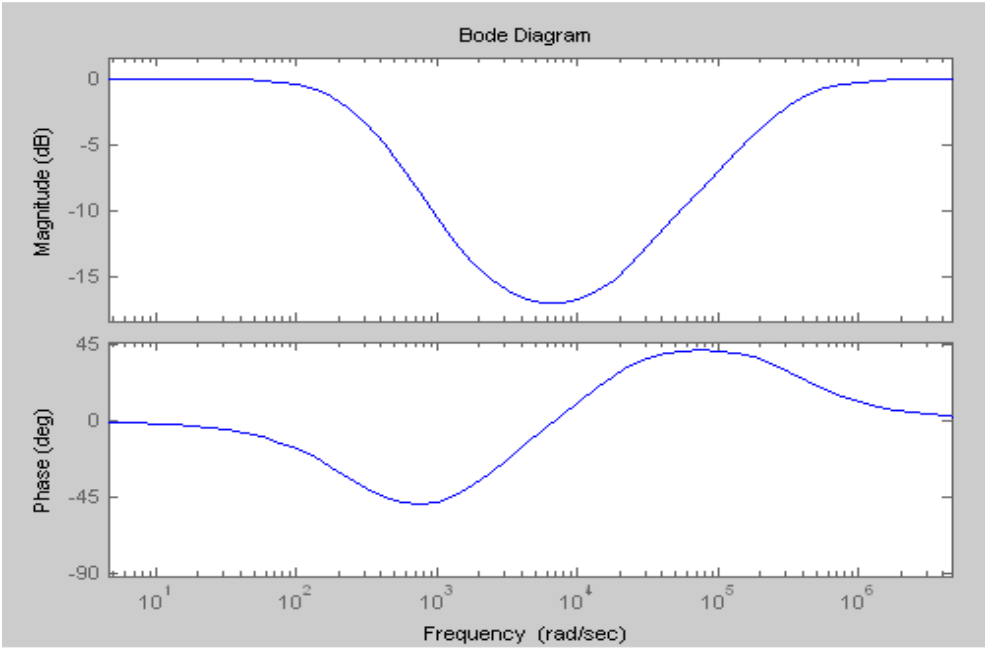

Figure 9: Matlab Simulation of Shallow Notch Filter

Combining the Shallow Notch Filter Transfer Function and the Microphone Transfer Function in open loop greatly reduced the initial peak of the microphone as seen below:

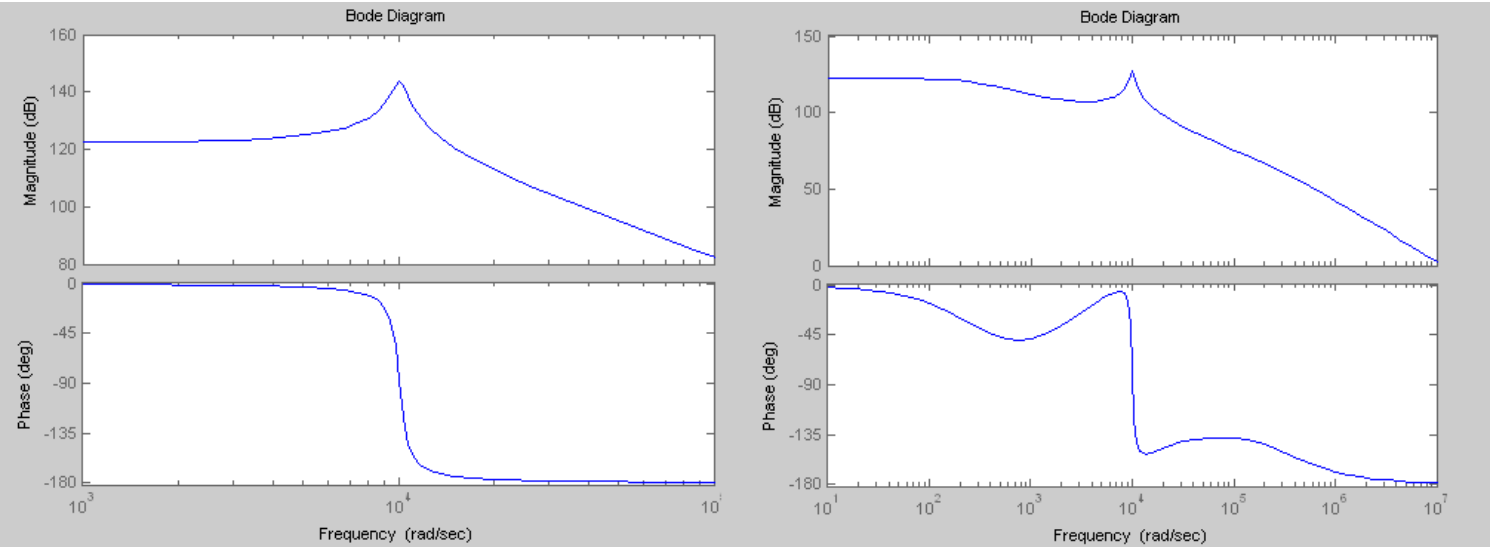

Figure 10: Left- Microphone Frequency Response Right-Microphone Frequency Response through Notch Filter

However, the filter introduced also greatly distorted the phase of the microphone. Before more analysis was done, it was found that a decrease in system bandwidth was a better solution to reduce the gain and the notch filter was abandoned.

VII. Differentiation via Feedback Integrator:

In an attempt to avoid the high gain necessary to implement the derivative control a feedback integrator approach is analyzed. The transfer function of the high pass filter previously mentioned can be implemented using the block diagram in Figure 11.

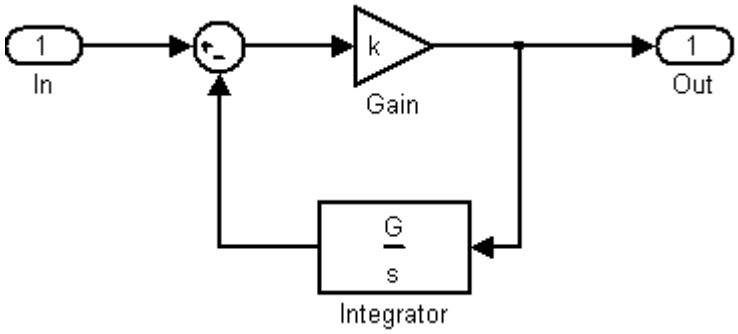

Figure 11: Feedback Integrator

The resulting transfer function for this system is:

$$\frac{V_{out}}{V_{in}} = \frac{k}{1+\frac{kG}{s}} \qquad (10)$$

which can be expressed as:

$$\frac{V_{in}}{V_{out}} = \frac{ks}{s+Gk} \qquad (11)$$

This transfer function is a single poled differentiator, or high pass filter, whose pole is $s = Gk$.

A possible circuit realization of this equation and its related transfer function can be seen in the figures below.

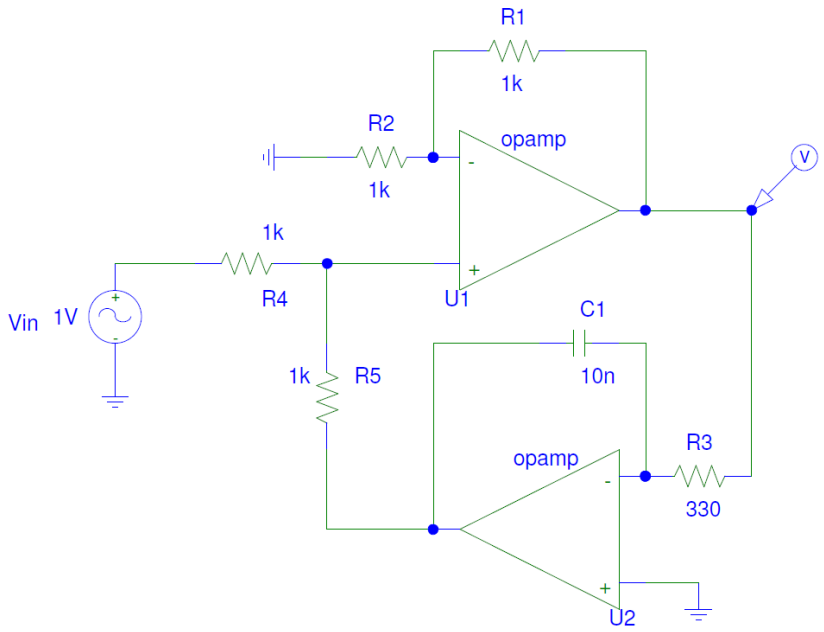

Figure 12: Realization of Feedback Integrator-Differentiator

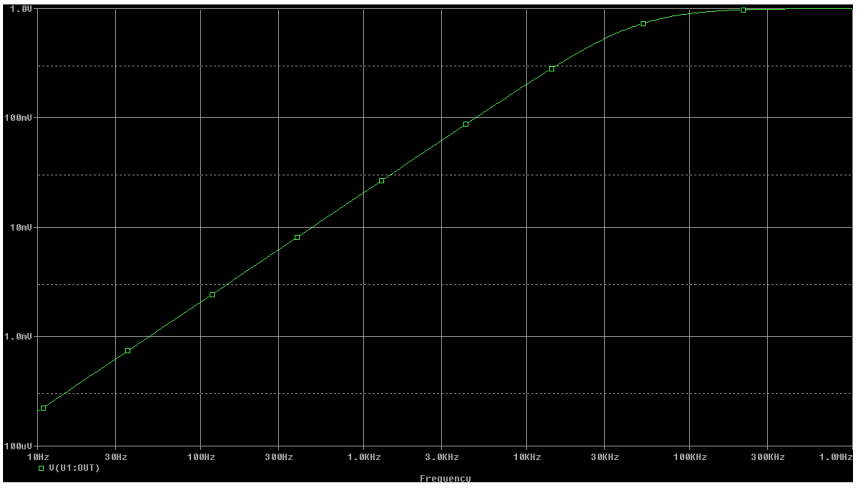

Figure 13: Transfer Function of Feedback Integrator-Differentiator

From end to end, this system still requires the same high gain that would be used for a simplified differentiator and would introduce additional phase delay into the system; however, the use of an integrator will quash some of the noise introduced by high frequency noise coming from the input of circuits that this will attach to because of the low pass filter frequency response of the integrator.

VIII. Noise Summary

Although noise can be calculated for the controller itself, research on noise was halted and stricken from the requirements after being informed that an essential element to the project

could not be obtained. Errors of manufacturing the MEMS microphone halted the production of a single unit MEMS microphone and laser vibrometer to be produced by Georgia Institute of Technology. The sensor to be used in this packaging takes advantage of the microphones low self noise and when combined with the microphone, they will have a lower noise floor than the laser vibrometer currently being used in Professor Ronald Mile's lab. This is not to say all of the noise research went to waste. The information gathered from the research was still used to make reasonable part selection but not to the extent to meet the noise requirement.

IX. PCB

An initial goal of this project was to create a PCB of the final circuit to be placed in a metal chassis. Testing of the final circuit revealed more variations in the parameters that were not initially taken into account. These variations lead to a last minute redesign of the circuit to incorporate the ability to switch the signs of the proportional and derivative gains. It was then advised by Professor Quang Su to not fabricate the PCB and instead keep the circuit on breadboard to allow future modifications to the circuit if needed.

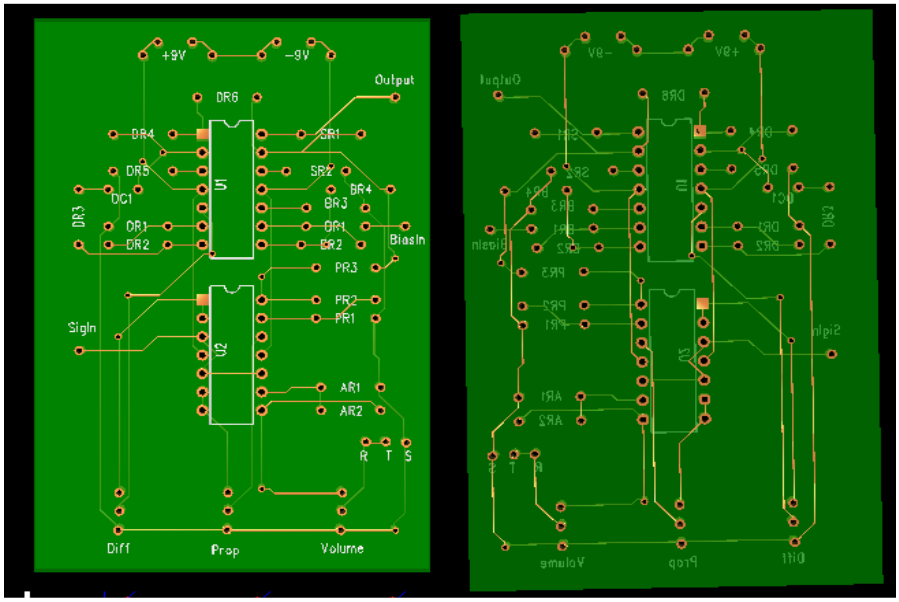

Figure 14:Latest PCB design before PCB implementation was abandoned

X. Chassis

A metal chassis was built to hold the PCB and two 9V batteries. It also allowed for input of the proportional input and bias voltage through BNC connectors as well as a BNC connection for the output of the controller.

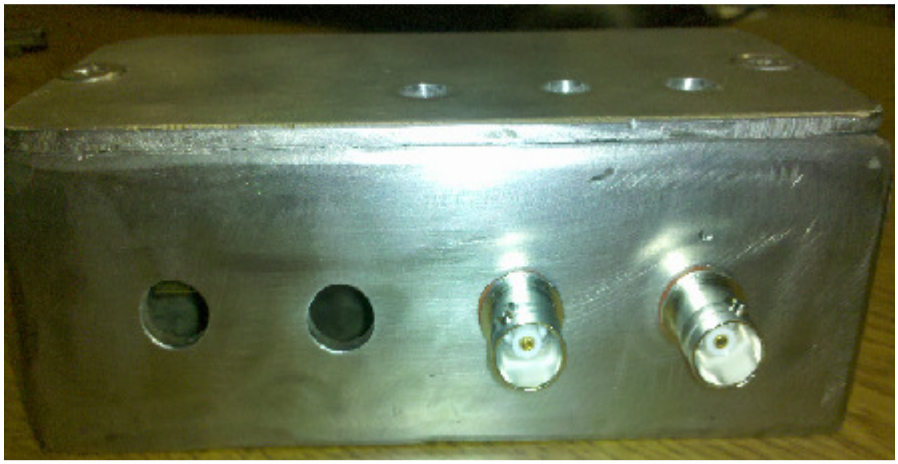

Figure 15. Metal Chassis designed for PCB

Since the PCB was no longer being fabricated, this box was also discarded. The circuit was now designed to be built on breadboard and a metal encasing around the breadboard was used.

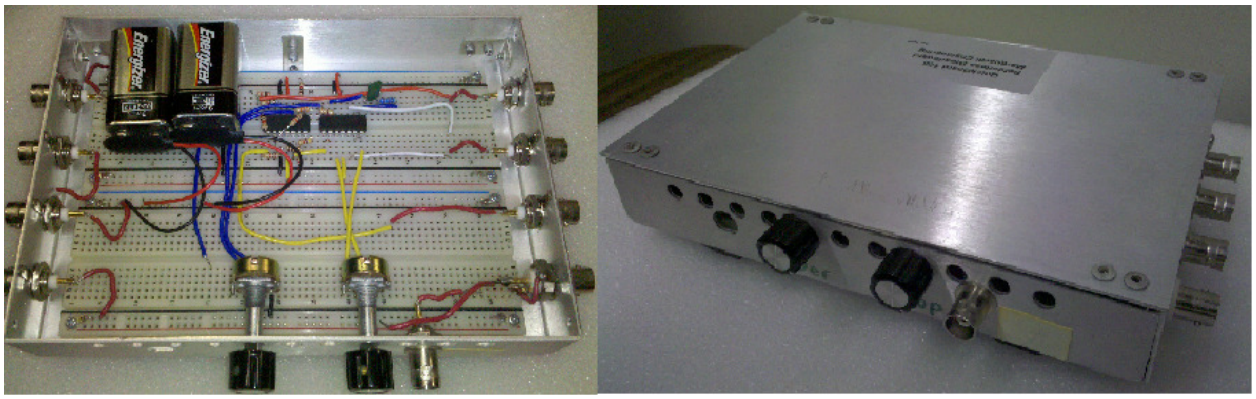

Figure 16: Metal Chassis used for bread board

BNC connectors were used to connect the bias voltage, proportional input signal, and output signal of the circuit since the testing equipment used had BNC connectors.

XI. Final Design

Reliability

Last semester, extensive parameters variations analysis was conducted to examine the effects on possible variations of the microphone. To summarize the findings from that study, the tensional stiffness, k_t, and mass moment of inertia, I, have the greatest effect on the system because both of the parameters control the natural frequency which the peak occurs. Unfortunately, since the derivative gain is set at a relatively low max the PD controller is not as tolerant to changes in the natural frequency as analysis predicted. This reduction in tolerance is strictly due to the constraints imposed by the maximum realistic gain.

To increase flexibility between microphones, switches were added to the proportional and derivative terms to allow sign changes. This is important feature to include because the feedback signal's sign could change depending on how the microphone responses to the change of capacitance with respect to the angle of deflection.

Social Impact

The driving force behind Professors Ronald Miles research is to greatly improve upon the current generation of hearing aids by using his MEMS microphone; however, the microphone is not limited to just hearing aids. The microphone has potential applications in sonar and law enforcement.

In the area of law enforcement, the microphone can replaced commonly used audio bugs. The low noise floor of the microphone and its high sensitivity makes it ideal for picking up quiet whispers with extreme clarity. The combined microphone and sensor when fully packaged can potentially be reduced to the size of a quarter, which can be placed anywhere with little notice.

Another possibility is using this microphone for sonar. Sonar is primarily used in the low frequency end of the aural spectrum. The noise at lower frequencies is higher than at higher frequencies because of pink noise which increases at a rate of 1/f. The low noise floor of the microphone combined with increased sensitivity of lower frequency allows for much more precise measurements and less power needed in order to pick up longer distanced signals.

The list of applications and societal benefits and applications is nearly endless. Wherever there is a microphone needed it can be replaced with this MEMS microphone. It is both more sensitive than anything currently available and it's frequency response is highly configurable in a wide variety of circumstances.

Economical Impact

The fabrication of these small delicate microphones is very expensive, time consuming, and difficult. Creating these microphones with a greater stiffness would also lower the frequency response peak; however, it would also lower the sound quality because the microphone will not move freely to sound pressure. Redesigning the microphones to do this will also take time and resources. A simpler solution to reducing the frequency response peak is to create additional circuitry to solve the problem.

XII. Final Electrical Circuit Design

Proportional

The proportional gain is created using a non-inverting op-amp configuration with resistor values of 1kOhm and 4.7kOhm to create a maximum gain of 5.7. The switch is used to toggle the sign of the gain.

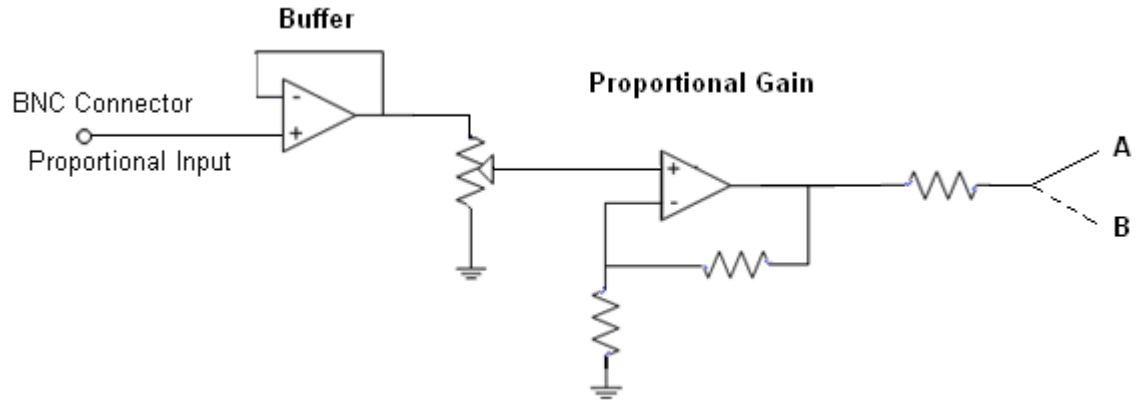

Figure 17: Proportional Gain Circuit

Differentiator Circuit Design

A pure differentiator has many realistic issues and thus a high pass filter is used in order to simulate differentiation over the frequency range of interest. Figure 18 is the op amp circuit that is described by equation 12. The cutoff frequency f_c is chosen to be slightly above the system bandwidth to minimize the required gain. The gain of 60 is created over two stages using a non-inverting op amp and a high pass filter. The non-inverting op amp is also a buffer and the potentiometer controls the input voltage level.

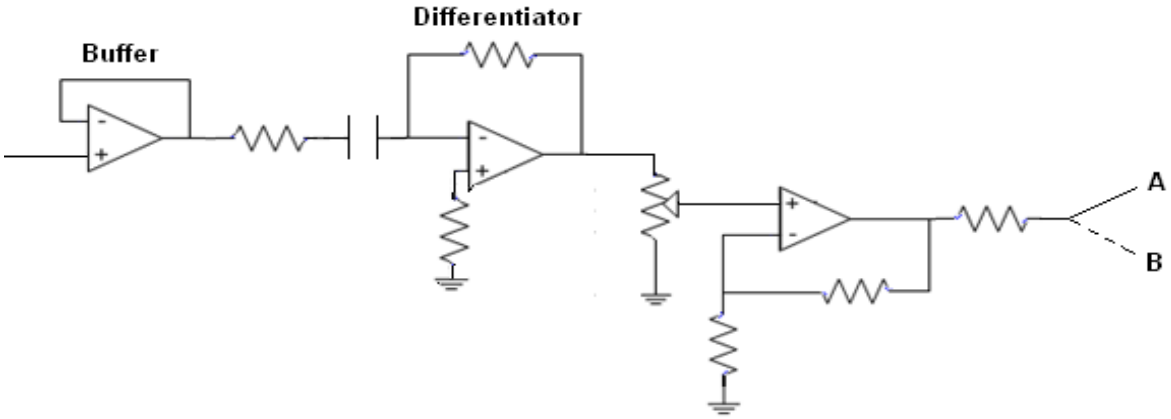

Figure 18: Differentiator Circuit

$$H_d(s) = \frac{K_d \cdot s}{s + 2\pi f_c} \quad (12)$$

Audio

The Audio Output Circuit is created using a non-inverting op amp configuration with resistor values of 1kOhm and 10kOhm to great a maximum gain of 11. The potentiometer after the amplifier allows for control of the volume of the output. The output is then connected to the Tip and Ring of the TRS 3.5mm audio jack.

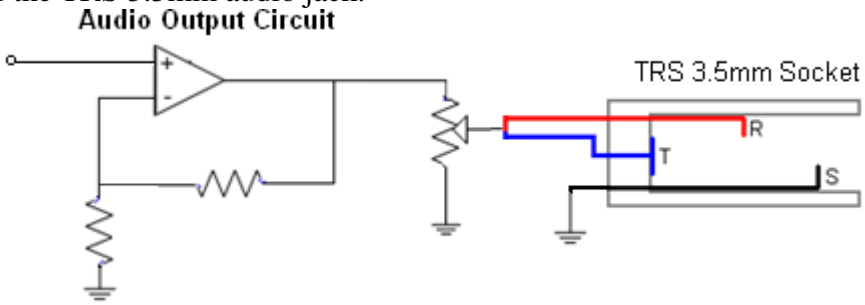

Figure 19: Audio Output Circuit configuration

Summer

The proportional and derivative gains are summed with the bias voltage input at the summer circuit. The circuit uses a difference amplifier. If a positive gain is wanted they are switched to "A" and if a negative gain is wanted, the switch is flipped to B.

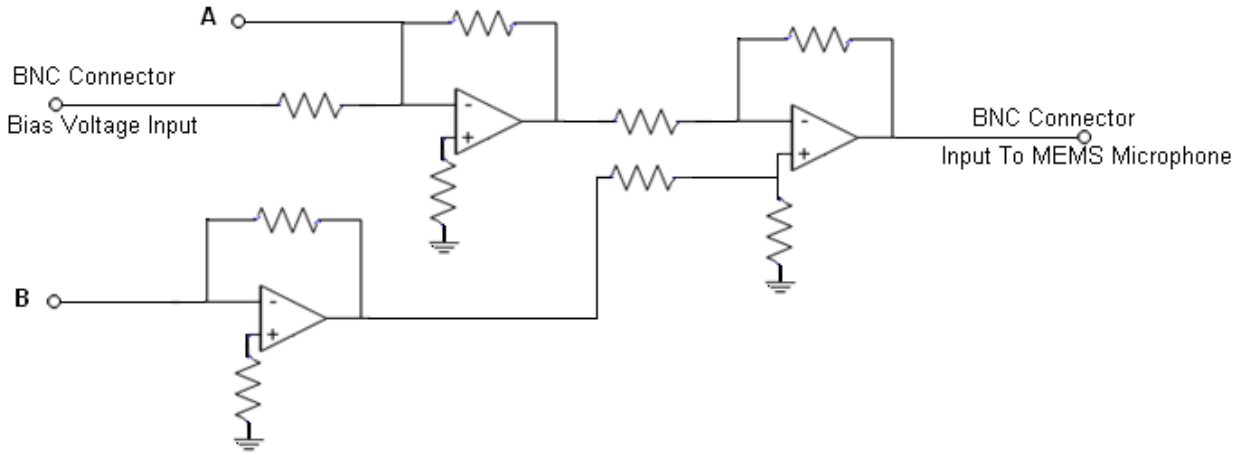

Figure 20: Summer Circuit

Final Cost

The final controller design requires three OP470 quad-package Op-Amps, various resistors, potentiometers and capacitors. Since the PCB fabrication was canceled, the total cost of the project was greatly reduced. In addition, the chassis was supplied to the project by the customer.

Item #	Item Name	P/N (if applicable)	Cost / unit	Quantity	Total Cost
1					$0.00
2	9v battery		$3.00	2	$6.00
3	10kOhm Potentiometers		$2.35	3	$7.05
4	Resistors (330 pcs)		$8.00	1	$8.00
5	Capacitors		$0.50	5	$2.50
6	OP470 Op Amp		$8.76	3	$26.28
7	Audio Jack 3.5mm 1/4"		$3.00	1	$3.00
			Total Materials		**$52.83**

XIII. Implementation Problems: Gain Bandwidth Product

Op-amps with high gain bandwidth products were chosen for this project because of the high gains that would be needed. However, the gain needed was still too large for the gain bandwidth product of the op-amps to contain the whole bandwidth of 20 kHz.

XIV. Testing and Results

1. Unit Testing

Summer Circuit

To test the Summer Circuit, the Op-Amps are powered with +/- 9V rails and the output is read on the oscilloscope. A function generator is set to a 1Vpp sine wave with a 1 kHz frequency. The power supply is also needed to output a constant 3V bias. The four test cases included connecting both signals to “A”, both signals to “B”, the constant 3V bias to “A” and the sinusoid to “B” and vice versa.

Results:

Both signals on “A” created a 1Vpp sine wave with a 3V offset. Connecting both signals on “B” created an inverted 1Vpp sine wave with a -3V offset. Placing the 3V bias on “A” and the 1Vpp sine wave on “B” created an inverted 1Vpp sine wave with a 3V offset. Placing the 1Vpp sine wave on “A” and the 3V bias on “B” created a 1Vpp sine wave with a -3V offset. These results are what were expected.

Differentiator Circuit

To test the Differentiator Circuit, the Op-Amps are powered with +/- 9V rails and the output is read on the oscilloscope. A 100mVpp sine wave is used as an input to the circuit and its frequency is incremented by 400 Hz for each data point. The amplitude and the phase of the

wave output from the Differentiator circuit would be compared with the theoretical frequency response calculated.

Results:

During testing of the differentiator circuit, a problem was encountered. When an input above 400mVpp was entered as an input, the output sinusoid created distortion as seen bellow:

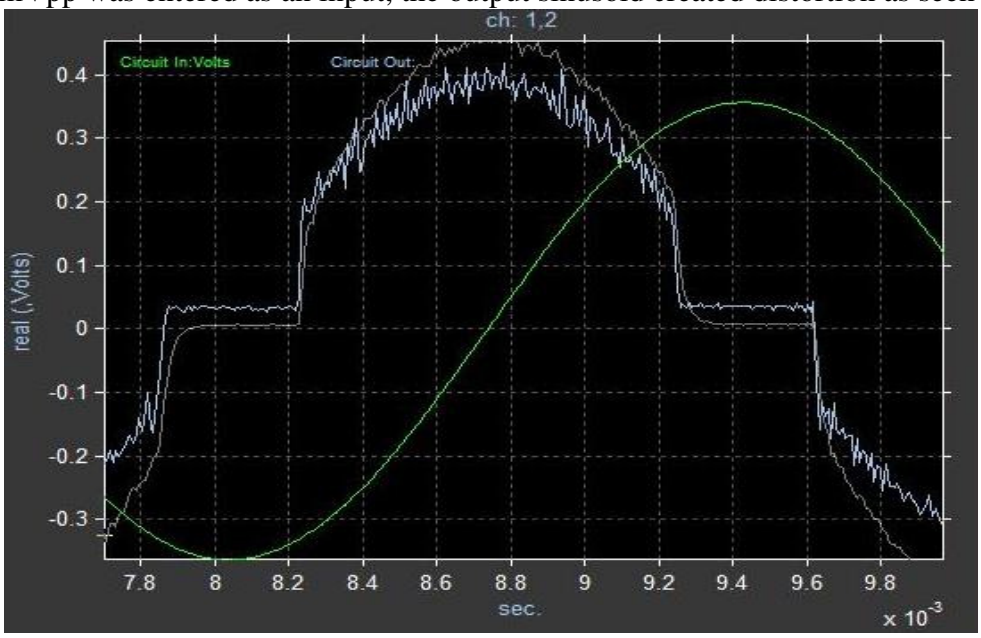

Figure 21: Distortion of Differentiator Output

This was caused by having the gain stage before the differentiator. The gain stage would cause the input to reach rail voltages. The differentiator differentiates a constant signal resulting in a voltage of 0. This problem was fixed by placing the differentiator before the gain stage.

The phase and amplitude at the chosen frequencies were very close to the calculated values. The graph below displays the actual results with the calculated results.

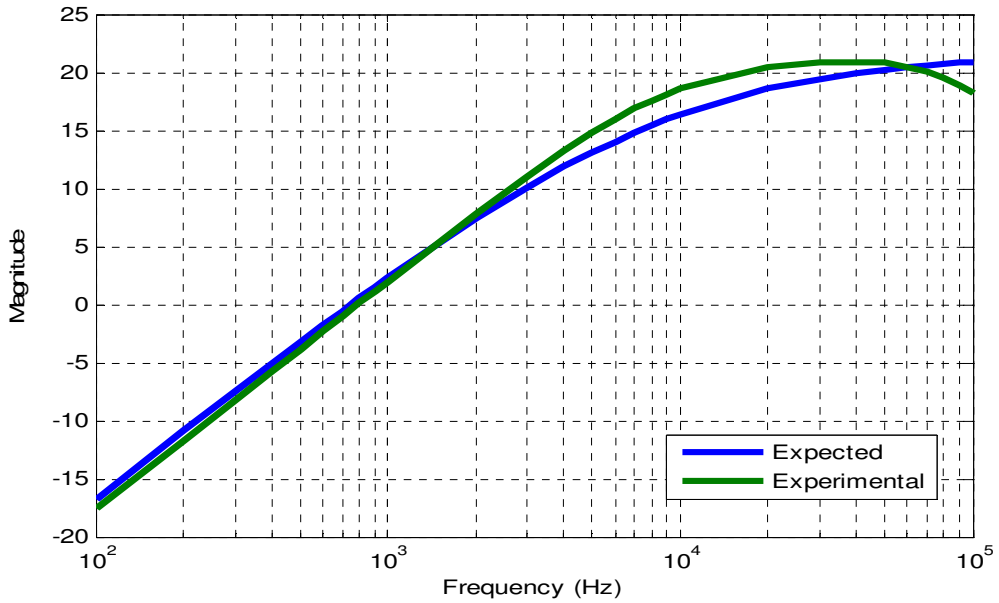

Figure 22: Differentiator Test Results

Proportional

To test the Proportional Circuit, the Op-Amps are powered with +/- 9V rails and the output is read on the oscilloscope. The potentiometer is turned to allow for highest gain and the input to the circuit is a 1Vpp sine wave with a 1 kHz frequency. The output is measured to ensure the gain is approximately 5.7. The frequency is also raised to 25 kHz to ensure the gain can remain stable to 20 kHz. The potentiometer is turned to ensure that gain can be lowered as well.

Results:

The gain of the circuit was as calculated and was stable up to 90 kHz.

2. System Integration

Before incorporating the plant into the system, the controller design was tested to verify the design. The input and output of the controller were monitored by a Data Acquisition System in Professor Ronald Miles Microacoustics lab.

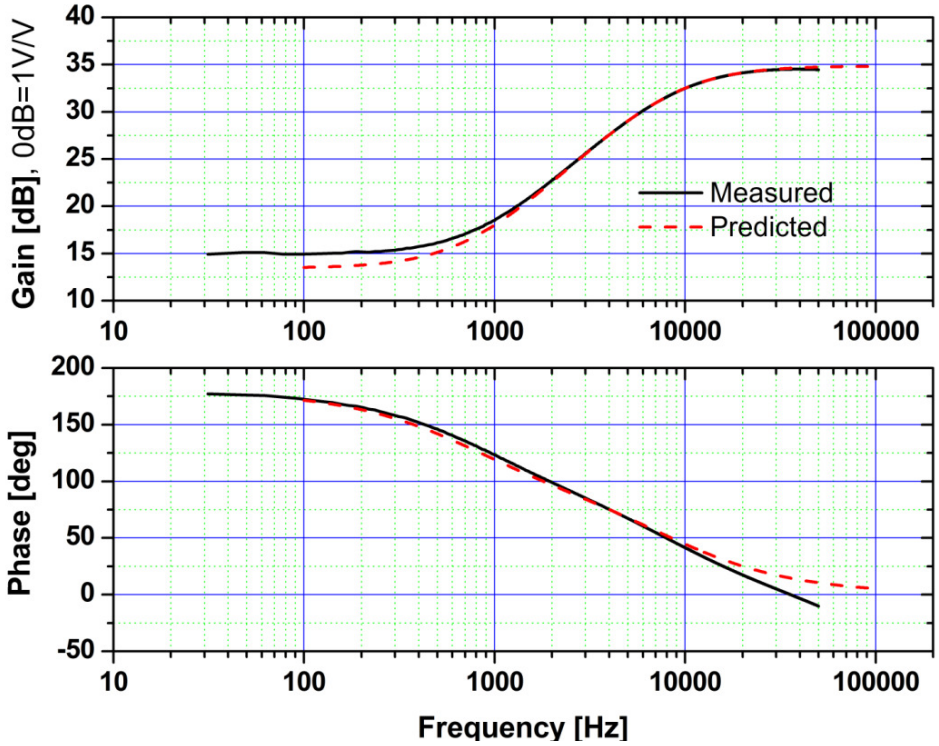

Figure 23: Controller Frequency Response

As can be seen in the diagram, the controller fits the predicted equation of $\frac{V_{out}}{Vin} = k_D s + kp$. Additional tests showed that as the frequency increased further the amplitude drops due to gain-bandwidth-product limitations. This was determined not to be an issue because the drop is significantly outside the frequency range of interest and therefore does not affect the controllers closed loop frequency response.

3. Customer Integration

The customer required the controller's input signal to come from a PolyTech laser-vibrometer. The laser-vibrometer's output is attached to the input of the feedback controller, which is powered by +/- 9V. The output of the controller is attached to a BNC connector that electrically connects to the interdigitated fingers of the MEMS microphone. In addition a 5 volt bias source was applied to the circuit to linearizing the control system. Inside the acoustical chamber housing the microphone, white noise is fed to the microphone to test the entire frequency spectrum of the microphone.

Results

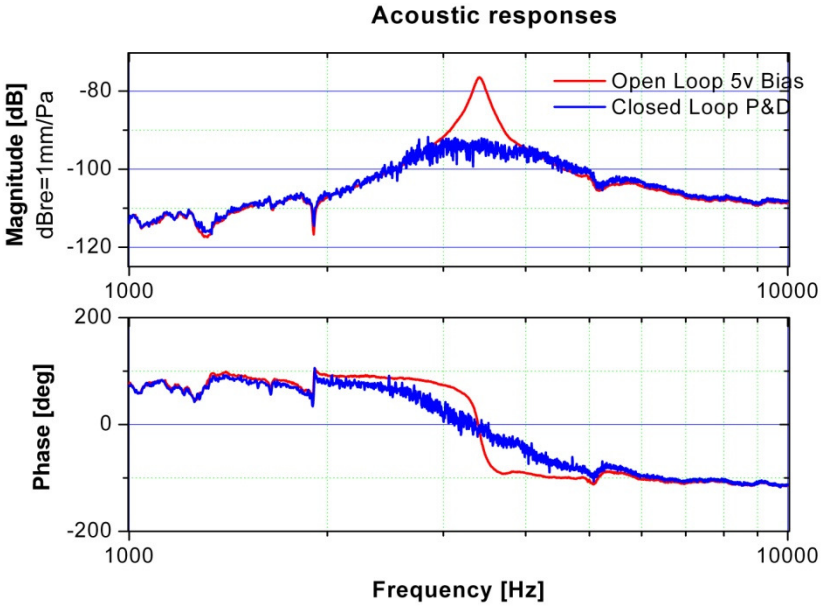

Figure 24: Frequency Response of Closed Loop System

As can be seen in the plot, the resonant frequency of the microphone tested at a 5V bias is around 3.4kHz. When the controller is attached, the peak of the closed loop system is significantly reduced; however, the bandwidth of the system is approximately 2 kHz, lower than desired. The only way to further reduce the peak, and increase bandwidth, is to increase the gain of the derivative term of the controller. The derivative gain cannot be increased without consideration to the system as a whole. By increasing the gain of the derivative term, the average amplitude of the control signal increase. If the control signal voltage exceeds or closely approach the DC bias voltage, the system becomes non-linear and the effectiveness of the controller can no longer be predicted.

XV. Requirements Matrix & Customer Sign Off

The overall project goal to reduce the peak in the frequency response of the microphone was a success. However, due to problems with testing equipment and the unexpected delay of the optical sensing mechanism from the Georgia Institute of Technology, some requirements were unable to be met or verified. The tested had to be completed using the laser-vibrometer which

had a large noise floor. Because of this, requirements such as “Filter shall only add up to 5dB of audible noise” could not be verified. Also, since the laser-vibrometer’s interface computer experienced technical difficulties, thorough testing of dynamic ranges and output clipping were also unable to be verified.

Project requirements that involved the building of a unit were met. The controller met its dimension, use of low noise parts, chassis, audio requirements, and most importantly, was able to reduce the microphone frequency response peak. Overall, the customer was satisfied with the results.

XVI. Schedule:

	Week of			22-Feb	1-Mar	8-Mar	15-Mar	22-Mar	29-Mar	5-Apr	12-Apr	19-Apr	26-Apr
Task Name	Responsible Party												
Implementing & Testing	Entire Team	Exp			10%	25%	45%	65%	75%	85%	100%		
		Act			0%	10%	25%	45%	75%	75%	75%	100%	
Summer Circuit test	Entire Team	Exp		50%	100%								
		Act		50%	100%								
Differenitator test	Entire Team	Exp			50%	100%							
		Act			35%	75%	100%						
Audio Output Test	Entire Team	Exp			50%	100%							
		Act			50%	100%							
Full Controller Test	Entire Team	Exp				50%	100%						
		Act				100%							
PCB Check	Entire Team	Exp						50%	100%				
		Act						50%	100%				
85dB Clipping Test	Entire Team	Exp							50%	100%			
		Act							X	X	X	X	X
55dB Dynamic Range Test	Entire Team	Exp						50%	100%				
		Act						X	X				
Closed Loop Stability Test	Entire Team	Exp							50%	100%			
		Act							50%	50%	75%	100%	
Noise Floor Test	Entire Team	Exp							50%	100%			
		Act							X	X			
Adjustable Gains Test	Entire Team	Exp				50%	100%						
		Act				50%	100%						

As can be seen on the schedule testing, there was a significant delays in testing. There several reasons behind these delays. First and foremost, there is limited access to the laser-vibrometer sensor which is needed for almost every aspect of testing. Access was usually limited to, at most, once a week. The week of 4/19 the sensor was inaccessible; both professors who allowed access to it were away at a conference. The second major issue is that the laser-vibrometer is legacy equipment, even though much of the hardware for the computer running it has been updated, it is very unreliable. Often the system will be inoperable for several hours as it needed to be continually rebooted until it became functional again. The week of 4/12 was lost due to the inoperability of the sensor.

Two weeks of testing were lost due to issues with realizing the circuit. The first issue was realizing practical gains for the differentiator part of the circuit. A couple redesigns were suggested, but instead the requirements for the project were changed to make the circuit possible. The second circuit issue came from building the full prototype of the circuit. The gain stages of the differentiator were placed in the wrong order; this caused the system voltage to clip before it was reduced causing the single to appear significantly distorted.

XVII. Conclusion

The goal of this project was to design a feedback controller that improved the frequency response of the closed loop system by reducing and potentially removing the resonant peak. Simulations conducted using pure differentiators proved to successfully set the closed loop poles, but using the physical system had some implementation issues that constrained the effectiveness of the feedback. The major implementation issue was the nonrealistic high pass filter gain required to produce the same control effect. Additionally, due to the bias point operation the feedback voltage fluctuations must be smaller than the bias voltage to avoid nonlinearities. These unavoidable constraints limit the possible effectiveness of an analog feedback controller. Additional tests should be conducted on microphones with a lower resonance to see the usefulness of the controller. These tests were not conducted during the semester due to the testing equipment going down and limited microphone availability.

From the testing conducted this semester it seems that the analog controller is not capable of entirely removing the peak. In order to remove the peak, additional control effort must be applied, but the amount of control effort is limited by the linearizing bias voltage. If the microphone could be linearized in a different fashion which allowed for more control effort, then the analog circuit might perform better. If another linearization method is not possible, other control schemes such as sigma-delta should be examined.

Refrences

"Twin-T Notch Filter Design Tool ". OKAWA Electric Design. April 23, 2010 <http://www.palomar.edu/dsps/actc/mla/mlainternet.html>.